Recognition of Blurred Images by the Method of Moments

Jan Flusser, Tomáš Suk, and Stanislav Saic

Abstract—**This correspondence is devoted to the feature-based recognition of blurred images acquired by a linear shift-invariant imaging system against an image database. The proposed approach consists of describing images by features that are invariant with respect to blur and recognizing images in the feature space. The PSF identification and image restoration are not requiered.**

A set of symmetric blur invariants based on image moments is introduced. A numerical experiment is presented to illustrate the utilization of the invariants for blurred image recognition. Robustness of the features is also briefly discussed.

I. Introduction

One of the most frequent tasks in image processing is the recognition of an image (or, more frequently, of an object on the image) against images stored in a database. Whereas the images in the database are supposed to be ideal, the acquired image represents the scene mostly in an unsatisfactory manner. Because real imaging systems as well as imaging conditions are imperfect, an observed image represents only a degraded version of the original scene. Blur is introduced into the captured image during the imaging process by such factors as diffraction, lens aberration, wrong focus, and atmospheric turbulence.

The widely accepted standard linear model [1] describes the imaging process by a convolution of an unknown original (or ideal) image $f(x, y)$ with a space-invariant point spread function (PSF) $h(x, y)$

$$g(x, y) = (f * h)(x, y) \tag{1}$$

where $g(x, y)$ represents the observed image. The PSF $h(x, y)$ describes the imaging system, and in our case, it is supposed to be unknown.

The classical "blind-restoration" approach to the recognition of blurred images consists of the following three steps:

- estimation of the PSF $h(x, y)$
- estimation of the ideal image $f(x, y)$ via restoration of the blurred image $g(x, y)$
- matching the restored image against an image database.

All these steps have been dealt with extensively in the literature during last two decades.

One group of methods for PSF identification is based on the investigation of zero patterns in the frequency domain [2]–[4] or spike patterns in the cepstral domain [5]. Another group of methods is based on modeling of the image by a stochastic process. The original image is modeled as an AR process and the blur as an MA process. The blurred image is then modeled as an ARMA process, and the MA process identified by this model is considered to be a description of the PSF. In this way, the problem of PSF estimation is transformed onto the problem of determining the parameters of an ARMA model [6]–[11].

Manuscript received April 24, 1994; revised July 7, 1995. This work was supported by Grant 102/94/1835 of the Grant Agency of the Czech Republic. The associate editor coordinating the review of this paper and approving it for publication was Dr. Reginald L. Lagendijk.

The authors are with the Institute of Information Theory and Automation, Academy of Sciences of the Czech Republic, Prague, Czech Republic.

Publisher Item Identifier S 1057-7149(96)01790-3.

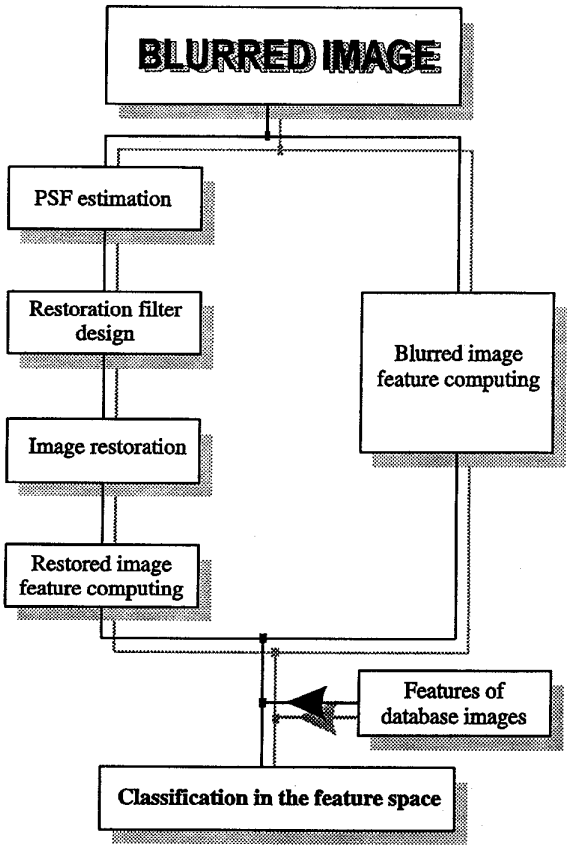

Fig. 1. Flowchart of a blurred image recognition process: a traditional approach (left stream) and a new approach (right stream).

After the PSF has been identified, the original image can be estimated via restoration of the blurred image by inverse filter, Wiener filter, or by any other similar technique (see [1], [12], or [13] for a survey). Finally, the restored image is compared with each image of the database to find the best match.

Generally speaking, the abovementioned approach to image recognition is very complicated and time consuming. In this paper, we present a completely different approach. The idea is quite simple: We describe all images (the blurred one as well as the images in the database) by a set of features, which are invariant to the blur (that means the feature values of $g(x, y)$ do not depend on $h(x, y)$, and they are the same as the feature values of $f(x, y)$) and can distinguish among the images. Image recognition is then accomplished via classification in the feature space. In this way, we get rid of the necessity of the PSF identification and image restoration (see the flowchart in Fig. 1).

Blur-invariant features introduced in this correspondence are based on image moments. In Section II, we deal with central moments of a blurred image, and we express them as functions of moments of an ideal image and the PSF. Then, our attention will be focused on the symmetric blur, which involves long-term atmospheric blur and out-of-focus blur as special cases. Section III contains the major part of the paper. An original algorithm for invariants derivation is

presented, and the invariants up to the fifth order are shown in the explicit form. Robustness of the invariants with respect to additive random noise is investigated in Section IV. Finally, the utilization of the invariants for recognition of blurred portrait photographs is experimentally demonstrated in Section V.

II. Moments of a Blurred Image

The 2-D $(p+q)$th-order *central moment* $\mu_{pq}^{(f)}$ of image $f(x,y)$ is defined by the integral

$$\mu_{pq}^{(f)} = \int_{-\infty}^{\infty}\int_{-\infty}^{\infty}(x-x_t^{(f)})^p(y-y_t^{(f)})^q f(x,y)\,dx\,dy \quad (2)$$

where $(x_t^{(f)}, y_t^{(f)})$ are the coordinates of the center of gravity of image $f(x,y)$.

The following theorem describes how to express moments of a blurred image in terms of moments of original image and PSF.

Theorem 1: Let $f(x,y)$ be a function describing an original image and $h(x,y)$ a shift-invariant PSF of a linear imaging system. The functions $f(x,y)$ and $h(x,y)$ are supposed to be piecewise continuous and nonzero only on bounded supports. Let $g(x,y)$ be a blurred image given by the convolution (1). Then, the relation

$$\mu_{pq}^{(g)} = \sum_{k=0}^{p}\sum_{j=0}^{q}\binom{p}{k}\binom{q}{j}\mu_{kj}^{(f)}\mu_{p-k,q-j}^{(h)}$$

holds for every p and q.

Using the definition of central moment (2) and the definition of convolution and changing the order of the integrals, we can easily prove the assertion of Theorem 1.

III. Symmetric Blur Invariants

In this section, we derive moment-based image features that are independent of blur, i.e., independent of the type and parameters of $h(x,y)$. Feature B is called *blur invariant* if and only if $B^{(f)} = B^{(f*h)} \equiv B^{(g)}$ for every $h(x,y)$.

We consider *symmetric* blur only, which means that $h(x,y)$ is assumed to be symmetric with respect to both axes and both diagonals

$$h(x,y) = h(-x,y) = h(y,x)$$

and, moreover, the degradation system is assumed to be energy preserving, i.e., $\mu_{00}^{(h)} = 1$. Note that every PSF with radial symmetry $h(x,y) = h(r)$ is a special case of symmetric blur defined above. Therefore, two very frequent types of blur—long-term atmospheric turbulence blur and out-of-focus blur—belong to our class of symmetric blur.

Lemma 1: If $h(x,y)$ satisfies the conditions of symmetry, then

- $\mu_{pq}^{(h)} = \mu_{qp}^{(h)}$ for every p, q;
- if p and/or q are odd, then $\mu_{pq}^{(h)} = 0$.

The proof of Lemma 1 is straightforward.

A. Derivation of the Invariants

Derivation of the invariants up to the third order is almost trivial. It is quite easy to prove by means of Theorem 1 and Lemma 1 that $\mu_{00}, \mu_{11}, \mu_{20}-\mu_{02}, \mu_{12}, \mu_{21}, \mu_{03}$ and μ_{30} are invariant with respect to symmetric blur.

We propose the following algorithm for the construction of symmetric blur invariants of any order:

1) Let μ_{pq} be any central moment, and let $p+q>1$. Then we start by setting

$$K = [(p+q-4)/2]$$

(symbol $[x]$ denotes an integer part of x)

$$I_0 = \mu_{pq}$$

if p and/or q are odd, and

$$I_0 = \mu_{pq} - \mu_{qp}$$

if p and q are even, and $p \neq q$. If p is even and $p = q$, no invariant is generated by the moment μ_{pq}.

2) **for** $n = 0$ **to** K

Define D_n as

$$D_n = I_n^{(g)} - I_n^{(f)}.$$

D_n has the form

$$D_n = \sum_{i=1}^{s_n} F_i(\mu^{(f)})\mu_{a_ib_i}^{(h)} + R_n(\mu^{(f)}, \mu^{(h)})$$

where $F_1, \cdots, F_{s_n}$ are functions of central moments of image $f(x,y)$ only, and $\mu_{a_ib_i}^{(h)}$ are central moments of the highest order of $h(x,y)$. No moment of $h(x,y)$ of the same order is contained in $R_n(\mu^{(f)}, \mu^{(h)})$. Moments of $g(x,y)$ were evaluated by means of Theorem 1. It holds that

$$a_1 + b_1 = a_2 + b_2 = \cdots = a_{s_n} + b_{s_n} = 2(K-n+1)$$

and, due to the symmetry of $h(x,y)$, all a_i and b_i are even for each n. Define I_{n+1} as

$$I_{n+1} = I_n - \frac{1}{\mu_{00}}\sum_{i=1}^{s_n} F_i(\mu)\mu_{a_ib_i}.$$

endfor

3) Define the invariant $B(p,q)$

$$B(p,q) = I_{K+1}.$$

B. Symmetric Blur Invariants in Recursive and Explicit Forms

The invariants derived by the above described algorithm can be also expressed in a recursive form as follows:

$$B(p,q) = \mu_{pq} - \alpha\cdot\mu_{qp} - \frac{1}{\mu_{00}}\sum_{n=0}^{K}\sum_{i=m_1}^{m_2}\binom{p}{t-2i}\binom{q}{2i} \cdot B(p-t+2i, q-2i)\cdot\mu_{t-2i,2i} \quad (3)$$

where

$$K = [(p+q-4)/2],$$
$$t = 2(K-n+1),$$
$$m_1 = \max(0, [(t-p+1)/2]),$$
$$m_2 = \min(t/2, [q/2]),$$
$$\alpha = 1 \Leftrightarrow p \wedge q \text{ are even},$$
$$\alpha = 0 \Leftrightarrow p \vee q \text{ are odd}.$$

TABLE I
Robustness of the Invariants with Respect to Additive Gaussian Zero-Mean Randon Noise. Top Row: Noise Standard Deviation; Middle Row: Signal-to-Noise Ratio (in Decibels); Bottom Row: The Distances Between the Original and Corrupted Images in 20-D Euclidean Feature Space

σ	0	5	10	15	20	25	30	35	40	45	50
SNR [dB]	-	26	21	17	15	13	11	10	9	8	7
$\varrho(f, g_\sigma)$ $[10^{-2}]$	0	0.2	0.3	0.5	0.9	1.0	0.8	1.5	1.4	1.1	1.9

(a) (b)

Fig. 2. (a) Original image; (b) image blurred by 21 × 21 smoothing mask and corrupted by additive Gaussian zero-mean random noise, SNR = 7 dB.

Note that if $(p \wedge q)$ are even, then the invariants $B(p,q)$ and $B(q,p)$ are dependent. Moreover, if $p = q$, then the invariant $B(p,q)$ computed by (3) is equivalent to some lower order invariant.

Applying the above described algorithm or (3), we can construct blur invariants of any order and express them in explicit form. A set of invariants of the fourth and fifth order is listed below:

- Fourth order:

$$B(1,3) = \mu_{13} - \frac{3\mu_{02}\mu_{11}}{\mu_{00}},$$
$$B(3,1) = \mu_{31} - \frac{3\mu_{20}\mu_{11}}{\mu_{00}},$$
$$B(4,0) = \mu_{40} - \mu_{04} - \frac{6\mu_{20}(\mu_{20} - \mu_{02})}{\mu_{00}}.$$

- Fifth order:

$$B(3,2) = \mu_{32} - \frac{3\mu_{12}\mu_{20} + \mu_{30}\mu_{02}}{\mu_{00}},$$
$$B(2,3) = \mu_{23} - \frac{3\mu_{21}\mu_{02} + \mu_{03}\mu_{20}}{\mu_{00}},$$
$$B(4,1) = \mu_{41} - \frac{6\mu_{21}\mu_{20}}{\mu_{00}},$$
$$B(1,4) = \mu_{14} - \frac{6\mu_{12}\mu_{02}}{\mu_{00}},$$
$$B(0,5) = \mu_{05} - \frac{10\mu_{03}\mu_{02}}{\mu_{00}},$$
$$B(5,0) = \mu_{50} - \frac{10\mu_{30}\mu_{20}}{\mu_{00}}.$$

Since the invariants should serve as features for image similarity or dissimilarity assessment, it is sometimes inconvenient to use directly the invariants described above.

The invariants should be normalized in two ways: to be independent of the image contrast and to have the same "weight" in the Euclidean metric space. To achieve this, we use *normalized blur invariants*

$$B'(p,q) = \frac{B(p,q)}{\mu_{00} \cdot (N/2)^{p+q}}$$

where N is the size of the image. It is also possible to use the normalization

$$B''(p,q) = \frac{B(p,q)}{\mu_{00}^{(p+q+2)/2}}.$$

In this way, we get the features invariant to the image scale but sensitive to the contrast.

IV. Robustness of the Blur Invariants

Every feature we want to use for image description and recognition should have the property of stability. Generally speaking, if two images are similar in some manner (in ℓ_2 norm for instance), then their feature values should be similar too, and vice versa. In this section, we will discuss how the blur invariants satisfy this criterion.

There are three different kinds of stability to be investigated in the case of blur invariants: stability under additive random noise (which is sometimes called *robustness*), stability with respect to boundary effect, and stability with respect to PSF distortions. In this correspondence, we discuss the robustness of the invariants only. Investigation of the influence of the remaining two factors will be the subject of future research.

Thus far, we have considered the noise-free model (1) only. Now, let us consider an imaging model with additive zero-mean (not necessarily Gaussian) random noise $n(x,y)$

$$g(x,y) = (f * h)(x,y) + n(x,y). \tag{4}$$

Since the image $g(x,y)$ is then a random field, all its moments and all invariants can be viewed as random variables. It holds that

$$E(\mu_{pq}^{(n)}) = E\left(\int_{-\infty}^{\infty}\int_{-\infty}^{\infty} x^p y^q n(x,y)\,dx\,dy\right)$$
$$= \int_{-\infty}^{\infty}\int_{-\infty}^{\infty} x^p y^q E(n(x,y))\,dx\,dy = 0$$

and

$$E(\mu_{pq}^{(g)}) = E(\mu_{pq}^{(f*h)}) + E(\mu_{pq}^{(n)}) = \mu_{pq}^{(f*h)}$$

where $E(X)$ denotes the mean value of random variable X.

In practice, however, only a single image $g(x,y)$ (i.e., only one realization of a random field) is available in most cases. We obtain

Fig. 3. Image database (first row: Eve, John, and George; second row: Kate, Catherine, and Lenka; third row: Mary, Mike, and Monica; fourth row: Petra, Stan, and Tom).

$\mu_{pq}^{(g)}$, but we are not able to estimate mean values $E(\mu_{pq}^{(g)})$. Since the moments are computed by a summation over the whole image, they are supposed to be affected by additive noise only very little. That means $\mu_{pq}^{(g)}$ are supposed to be close to $E(\mu_{pq}^{(g)})$, and we can directly use $\mu_{pq}^{(g)}$ for the computation of the invariants.

Accuracy of such a description is illustrated by the following experiment. Denote a blurred image corrupted by additive Gaussian zero-mean noise with standard deviation σ as $g_\sigma(x, y)$

$$g_\sigma(x, y) = (f * h)(x, y) + n_\sigma(x, y).$$

Robustness of the invariants up to the given order r is characterized by the distance $\varrho(f, g_\sigma)$ as a function of σ in the Euclidean space of invariants:

$$\varrho(f, g_\sigma) = \sqrt{\sum_{p+q \le r} (B'^{(f)}(p, q) - B'^{(g_\sigma)}(p, q))^2}.$$

The results in the case of Lena image are shown in Table I. In this experiment, image blur was introduced by an averaging of a 21×21 mask (the original image size was 256×256 pixels), and the noise had standard deviations σ from 5 to 50. The corresponding signal-to-noise ratio values defined as

$$\text{SNR} = 10 \cdot \log_{10} \cdot \frac{E((f * h)^2(x, y))}{\sigma^2}$$

were from 26 to 7 dB. In this experiment, the invariants $B'(p, q)$ up to the sixth order were utilized.

You can see that the robustness of the invariants is sufficiently high; even for the most corrupted image (which is degraded very heavily for human vision; see Fig. 2) the distance from the original is about 0.02, whereas the distances between Lena and other portrait images are usually higher than 1. Note that $\varrho(f, f * h)$ is approximately zero—this illustrates the invariance of the features.

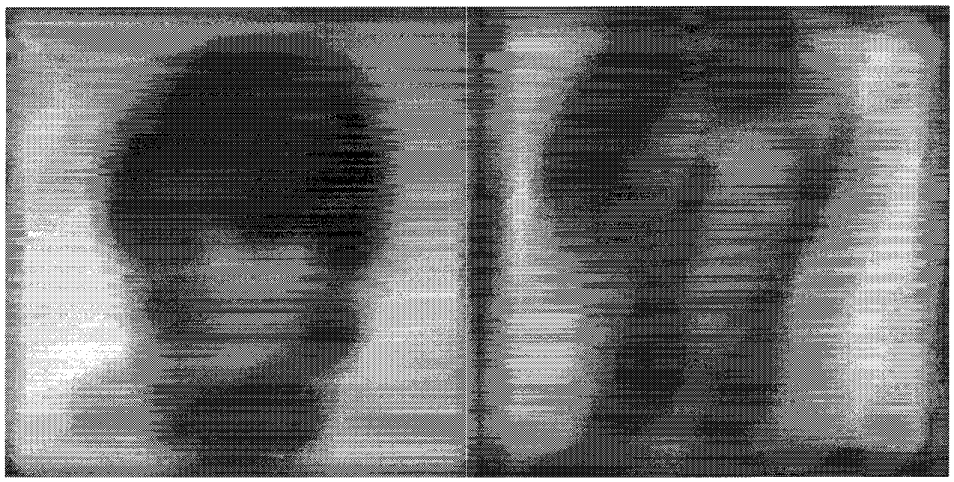

Fig. 4. Faces to be recognized: Person X (left) and Person Y (right).

V. Recognition of Blurred Images Against a Database: An Experiment

The experiment demonstrates the recognition of images degraded by a symmetric blur against an image database. The database of portrait photographs is shown in Fig. 3 (first row: Eve, John and George; second row: Kate, Catherine and Lenka; third row: Mary, Mike and Monica; fourth row: Petra, Stan and Tom). The size of each image is 256×256 pixels.

Two blurred images of unknown persons are displayed in Fig. 4 (Person X and Person Y). In fact, Person X is Catherine, and the photo in Fig. 4 is a defocused version of her photo from the database. Person Y is Eve, but her photograph in Fig. 4 is different from that in the database—it was taken about two years later.

The values of all invariants $B'(p,q)$, where $p+q \leq 6$, were calculated for each image. However, in the case of digital image f_{ij} of the size $N \times N$, we have to use a discrete approximation of (2) for moment evaluation:

$$\hat{\mu}_{pq} = \sum_{i=1}^{N} \sum_{j=1}^{N} (i - x_t)^p (j - y_t)^q f_{ij}. \tag{5}$$

Then, the unknown images were classified according to minimum distance rule in 20-D Euclidean feature space. The distances between each unknown image and the database elements are shown by a diagram in Fig. 5. As you can see, Person X as well as Person Y were recognized correctly.

The correct recognition of Person X is not a surprise—it follows immediately from the theory. However, successful recognition of Person Y cannot be generalized. We do not claim that our method is invariant to such things as hair color/style, aging, etc.

VI. Conclusion

This correspondence was devoted to the feature-based recognition of blurred images. The images were assumed to be formed by a linear shift-invariant imaging system, where the blur can be modeled by convolving an original image with a system point spread function. The proposed approach consists of describing images by the features that are invariant with respect to blur (that means with respect to the PSF) and recognizing images in the feature space. In comparison with complicated and time-consuming "blind-restoration" approach, we got rid of the necessity of the PSF identification and image restoration. Thanks to this, our approach is much more effective.

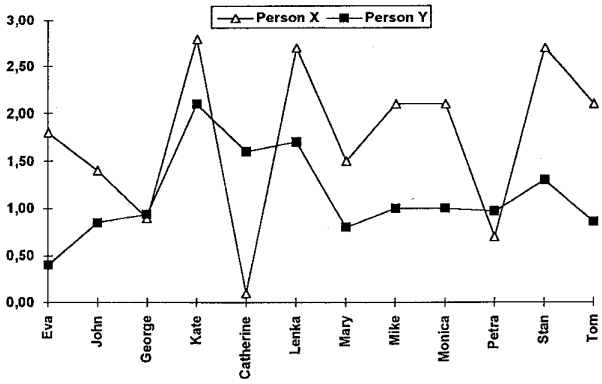

Fig. 5. Distances in the space of invariants between the unknown persons and the database images.

A set of features that are based on image moments and are invariant with respect to symmetric image blur was introduced in this correspondence. An original algorithm for the construction of the invariants of any order was presented, which is the major theoretical result of this work. The invariants proved to be sufficiently robust.

A numerical experiment was performed to illustrate the utilization of the invariants for blurred image recognition. However, our method has several limitations. The most significant limit arises from the fact that the image to be recognized should have roughly the same background as the images in the database.

References

[1] W. K. Pratt, *Digital Image Processing*, 2nd ed. New York: Wiley, 1991.

[2] D. B. Gennery, "Determination of optical transfer function by inspection of frequency-domain plot," *J. Opt. Soc. Amer.*, vol. 63, pp. 1571–1577, 1973.

[3] T. G. Stockham Jr., T. M. Cannon, and R. B. Ingebretsen, "Blind deconvolution through digital signal processing," *Proc. IEEE*, vol. 63, pp. 678–692, 1975.

[4] M. M. Chang, A. M. Tekalp, and A. T. Erdem, "Blur identification using the bispectrum," *IEEE Trans. Acoust., Speech, Signal Processing*, vol. 39, pp. 2323–2325, 1991.

[5] T. M. Cannon, "Blind deconvolution of spatially invariant image blurs with phase," *IEEE Trans. Acoust., Speech, Signal Processing*, vol. ASSP-24, pp. 58–63, 1976.

[6] A. K. Jain, "Advances in mathematical models for image processing," *Proc. IEEE*, vol. 69, pp. 502–528, 1981
[7] A. M. Tekalp, H. Kaufman, and J. W. Woods, "Identification of image and blur parameters for the restoration of noncausal blurs," *IEEE Trans. Acoust., Speech, Signal Processing*, vol. 34, pp. 963–972, 1986.
[8] R. L. Lagendijk, J. Biemond, and D. E. Boekee, "Identification and restoration of noisy blurred images using the expectation-maximization algorithm," *IEEE Trans. Acoust., Speech, Signal Processing*, vol. 38, pp. 1180–1191, 1990.
[9] S. J. Reeves and R. M. Mersereau, "Blur identification by the method of generalized cross-validation," *IEEE Trans. Image Processing*, vol. 1, pp. 301–311, 1992.
[10] A. E. Savakis and H. J. Trussel, "Blur identification by residual spectral matching," *IEEE Trans. Image Processing*, vol. 2, pp. 141–151, 1993.
[11] G. Pavlovic and A. M. Tekalp, "Maximum likelihood parametric blur identification based on a continuous spatial domain model," *IEEE Trans. Image Processing*, vol. 1, pp. 496–504, 1992.
[12] H. C. Andrews and B. R. Hunt, *Digital Image Restoration.* Englewood Cliffs, NJ: Prentice-Hall, 1977.
[13] M. I. Sezan and A. M. Tekalp, "Survey of recent developments in digital image restoration," *Opt. Eng.*, vol. 29, pp. 393–404, 1990.

Nonlinear Dynamic Range Transformation in Visual Communication Channels

Rachel Alter-Gartenberg

***Abstract*— This correspondence evaluates nonlinear dynamic range transformation in the context of the end-to-end continuous-input/discrete-processing/continuous-display imaging process. Dynamic range transformation is required when we have the following:**

- **i) The wide dynamic range encountered in nature is compressed into the relatively narrow dynamic range of the display, particularly for spatially varying irradiance (e.g., shadow).**
- **ii) Coarse quantization is expanded to the wider dynamic range of the display.**
- **iii) Nonlinear tone scale transformation compensates for the γ correction in the camera amplifier.**

I. Introduction

The performance of an image-gathering device is constrained by its optical response, sampling passband, and sensitivity. These constraints limit the resolution of the displayed image to the sampling interval and its visual quality to the level of degradations caused by acquisition, quantization, transmission, digital filtering, and display (Fig. 1). The tradeoffs among these degradations have been studied by Schreiber [1] for optimal design of electronic imaging, by Huck *et al.* [2] for optimal design of image gathering and digital restoration, and by Alter-Gartenberg [3] for constrained transmission. While linear modeling of the continuous-input/discrete-processing/continuous-display (c/d/c) imaging process inherently assumes homogeneous wide-sense stationary stochastic fields, this assumption does not apply to targets with spatially varying irradiance. Additionally, in most conventional acquisition systems, the nonlinear characteristic of the CRT display is gamma corrected at the camera amplifiers, i.e., at the transmitter, and not at the receiver [4]. For electronic imaging, the placement of this transformation does not affect the visual quality of the image. However, when digital image processing is added and the source of digital data comes from either conventional acquisition devices or digitized films, the gamma correction or the nonlinearity of the film exposure should be accounted for by a nonlinear dynamic range transformation.

This correspondence assesses the proper placement of the nonlinear dynamic range transformation in the context of the c/d/c/ imaging model. Design candidates for this assessment are informationally optimized image-gathering devices and optimal digital restorations, where the quantization process is part of the design of the analog-to-digital (A/D) converter [3]. The nonlinear transformation chosen for this assessment is a stochastic extension of the modified logarithmic transformation [5]> This extension accounts not only for false contours in coarse quantization [5] but also for dynamic range compression and expansion. The visual quality of the resultant image is compared with its corresponding linear compression and extension for both stationary and nonstationary fields. Three cases are addressed: dynamic range compression of spatially varying irradiance, dynamic range expansion from coarse-to-fine quantization, and tone-scale transformation to compensate for the γ correction.

Manuscript received September 19, 1993; revised December 21, 1994. This work was supported by NASA Task Assignment NAS1-18584-90 with the Department of Mathematics, Old Dominion University, Norfolk, VA 23529 USA. The associate editor coordinating the review of this paper and approving it for publication was Prof. Rama Chellappa.

The author is with the Computer Science Department, College of William and Mary, Williamsburg, VA 23187 USA.

Publisher Item Identifier S 1057-7149(96)01805-2.

II. Formulations

The formulations are given in both the spatial and the spatial-frequency domains. For presentation uniformity, discrete signals and functions are defined in their continuous representations. The symbols $\wedge$ and $\sim$ represent Fourier transforms of continuous (aperiodic) and discrete (periodic relative to sampling passband $\widehat{\mathbf{B}}$) signals, respectively. Consequently, the formulations distinguish between continuous and discrete processes and between periodic, bandlimited, and aperiodic signals and operations.

A. The End-to-End Visual Communication Model [2]

Digital image gathering ia characterized by its optical response $\tau(x,y)$ and sampling lattice $\underline{|||}$. It converts the *continuous* target $L(x,y)$ into the *discrete* signal $s(x,y)$

$$s(x,y) = [K\,L(x,y) * \tau(x,y)]\underline{|||} + n(x,y)$$

with a spatial–frequency response given within its sampling passband $\widehat{\mathbf{B}}(v,\omega)$ by

$$\tilde{s}(v,\omega) = [K\widehat{L}(v,\omega)\hat{\tau}(v,\omega)] * \underline{\hat{|||}} + \tilde{n}(v,\omega) \tag{1}$$

where

- K steady-state gain of the radiance-to-analog (R/A) signal conversion,
- $n(x,y)$ additive *discrete* photodetector noise.

The A/D converter quantizes $s(x,y)$ into $s_e(x,y)$ with a data density of $\eta = \log_2 \kappa$ bits over the dynamic range of $(-\sqrt{3}\sigma_s, \sqrt{3}\sigma_s)$

$$\sigma_s^2 = \iint\limits_{\widehat{\mathbf{B}}} \left\{[\widehat{\Phi}_L(v,\omega)|\hat{\tau}(v,\omega)|^2] * \underline{\hat{|||}} + \tilde{\Phi}_n(v,\omega)\right\} dv\,d\omega \tag{2}$$

where $\widehat{\Phi}_L(v,\omega)$ and $\tilde{\Phi}_n(v,\omega)$ are the target and noise power spectral densities (psd's), respectively. Signal values outside this range are assigned to either 0 or $\kappa - 1$.